Augmented State Estimation of Line Parameters in Active Power Distribution Systems With Phasor Measurement Units

Yubin Wang, Mingchao Xia, *Senior Member, IEEE*, Qiang Yang, *Senior Member, IEEE*, Yuguang Song, *Graduate Student Member, IEEE*, Qifang Chen, *Member, IEEE*, and Yuanyi Chen

***Abstract*—The line parameters of power distribution systems stored in the dispatching center may have large errors due to the line aging and system operational dynamics. Such line parameter errors may directly affect the state estimation accuracy, and the advanced management functionalities rely on these parameters. This paper proposes an augmented state estimation method of erroneous distribution line parameters considering the presence of phasor measurement units (PMUs). The augmented state-space models under single and multiple measurement snapshots are established separately by combining the parameter state equation with the state-space model of the distribution network. The augmented state estimation based on the improved adaptive unscented Kalman filter (IAUKF) is developed. The proposed method can effectively perceive the process noise statistical parameter of the erroneous parameters during the estimation to accurately estimate line parameters. The proposed solution is validated through simulation experiments using the IEEE 33-bus system and the numerical results demonstrated its accurate parameter estimation performance.Also, the scalability of the proposed algorithm is demonstrated based on the simulation of the 118-bus system with distributed generators.**

***Index Terms*—Distribution line parameters, augmented state estimation, improved adaptive unscented Kalman filter.**

I. Introduction

In recent years, a massive number of small-scale distributed generations (DGs), such as wind turbines (WTs), combined heat and power (CHP), photovoltaic sources (PVs) and new forms of power demand (e.g., electric vehicles) are being connected to the medium voltage (MV) distribution networks [1]. The power generation from these generators is often intermittent and brings about direct operation and control challenges on grid (e.g., frequent bidirectional power flows, protection degradation, and altered transient stability). The performance of the distribution management system (DMS) functionalities strongly relies on the accurate state estimation (SE). Therefore, to improve the safety and reliability of the distribution network operation, as well as the consumers' power quality, a highly accurate SE is required to obtain the awareness of the distribution network operation in a real-time manner [2]. The line parameters (resistance and reactance) are essential components of the state estimator [3], [4]. Consequently, the errors of the line parameters may lead to a permanent negative impact on the results of SE and mislead the DMS applications [5]. Also, the line parameters are essential in almost all power system analysis tools (e.g., relay protection configuration, reactive power optimization, operation control, and line loss management).

The line parameters stored in the dispatching center database are generally calculated by referring to the blueprint or planning document. The actual line parameters may deviate significantly from the theoretical ones without considering the impact of temperature, soil resistivity, and aging problems in the actual operation [6], [7]. Besides, the human-related factors, such as inaccurate manufacturing data and construction errors, as well as the inaccurate calculation of line lengths may lead to significant errors of the line parameters [5]. In addition, the accurate line parameters at the connections between cables and the overhead lines are hardly obtained in practice due to the complex structures. The line parameters stored in the database may be obsolete and erroneous, as confirmed by the previous study [8] that the errors of line parameters might reach up to 30%. Hence, it is of paramount importance to identify the erroneous line parameters in the database and estimate their precise values for future distribution network operation [9].

Substantial research has existed with regard to the identification of erroneous parameters by using the regularized residuals calculated by the weighted least squares (WLS) based SE (e.g., [10]–[12]). On the other hand, the conventional solutions of parameter estimation mainly include theoretical calculation method based on Kirchhoff's law and Ohm's law [7], [13], residual sensitivity analysis method [14]–[16] and WLS-based augmented state estimation method [17]–[19] whose procedure and principle were described in detail in [5]. The majority of the

Manuscript received 18 July 2021; revised 23 October 2021; accepted 18 December 2021. Date of publication 24 December 2021; date of current version 23 September 2022. This work was supported in part by the National Natural Science Foundation of China under Grant 52177119, in part by the Fundamental Research Funds for the Central Universities (Zhejiang University NGICS Platform), and in part by the Fundamental Research Funds for the Central University under Grant 2018JBZ004. Paper no. TPWRD-01076-2021.
(Corresponding author: Qiang Yang.)

Yubin Wang, Qiang Yang, and Yuanyi Chen are with the College of Electrical Engineering, Zhejiang University, Hangzhou 310027, China (e-mail: wang_yb@zju.edu.cn; qyang@zju.edu.cn; chenyuanyi@zju.edu.cn).

Mingchao Xia, Yuguang Song, and Qifang Chen are with the College of Electrical Engineering, Beijing Jiaotong University, Beijing 100044, China (e-mail: mchxia@bjtu.edu.cn; 16121517@bjtu.edu.cn; chenqf@bjtu.edu.cn).
Color versions of one or more figures in this article are available at https://doi.org/10.1109/TPWRD.2021.3138165.

Digital Object Identifier 10.1109/TPWRD.2021.3138165

above studies are relatively mature methods applied in the field of transmission line parameters estimation. There are also plenty of other researches that only focus on the transmission line parameters estimation [20]–[22]. The structure of the distribution network, which is different from the transmission network ones, is usually radial [3]. And, the line resistance cannot be ignored in the distribution network compared with the transmission network [23].

The measurement for line parameters estimation of distribution network mainly comes from the hybrid measurement of supervisory control and data acquisition (SCADA) and micro phasor measurement unit (μPMU) [9]. The SCADA can measure active/reactive power as well as voltage amplitude on buses, while the μPMU can provide voltage angle measurement on buses using GPS signals [24]. The relevant applications, such as system state awareness, event detection and auxiliary operation, based on the PMU for the distribution network, are developed rapidly in recent years [25]. Several approaches have been developed for line parameters estimation of distribution networks. For instance, a two-step framework approach that consists of a data-driven regression method and a joint data-and-model-driven method (i.e., a specialized Newton-Raphson iteration and power flow equations) was proposed in [9]. A data-driven method for parameters estimation in distribution grids was proposed in [26]. In [27], a reweighted nonlinear least-squares method was used to perform line parameters estimation. A line parameters estimation model of the distribution network was established with the least square method based on the PMU, which was solved by the Newton iteration method. In [28] and [29], the PMU measurements were utilized to achieve line parameters estimation. However, these methods involve iterations in the solution process. The significant difference between the accuracy of SCADA and PMU, and the extended dimension of the augmented state vector may result in the numerical problem of non-convergence. With the development of machine learning, there emerged attempts to use CNN for the identification of distribution network parameters [30]. However, there is still a lack of high-quality training datasets. Dynamic state estimation of power system is a recursive method that could obtain the estimation results without iterations, therefore there is no problem of non-convergence in the iterative. And its typical algorithm unscented Kalman filter (UKF) [31] has been widely used in the field of synchronous generator and dynamic load parameters estimation [32]–[35].

This paper develops a estimation method of distribution network line parameters by augmenting the state estimation. The technical contributions can be summarized as follows:

1) The augmented state-space model is established by combining the parameter state equation formulated according to the time-invariant characteristics of the parameters and the state-space model considering the suspicious parameters. Furthermore, the model is extended to the form under multiple measurement snapshots to improve the measurement redundancy since the parameters can be estimated off-line.

2) The improved adaptive UKF (IAUKF) is adopted for augmented state estimation. The noise statistic estimator (NSE) of IAUKF can accurately perceive the process noise statistical parameters which ensures the recursive estimation of suspicious parameters.

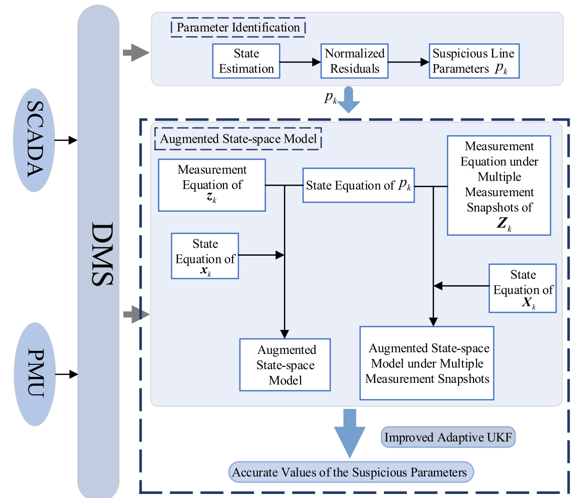

Fig. 1. Framework of the proposed solution.

3) The proposed approach is implemented and extensively validated through simulations. The numerical results obtained from the IEEE 33-bus system confirm its excellent estimation performance. The scalability and robustness of the proposed method are further demonstrated in the case of 118-bus system with DGs in the presence of bad measurement data.

The remainder of the paper is organized as follows. Section II overviews the proposed solution. Section III briefly introduces the IAUKF. The augmented state-space models of active distribution systems with PMUs under single and multiple measurement snapshots are presented in Section IV. Section V validates the performance and presents the numerical simulation results. In Section VI, the whole work of this paper is summarized and discussed.

II. Overview of the Proposed Solution

The framework of the method proposed in this study is illustrated in Fig. 1. The DMS can run the application of SE after receiving the measurement data from the SCADA and the PMU. Then the suspicious line parameters can be determined through the analysis of the measurement normalized residuals calculated based on the results of SE. The accurate values of the suspicious line parameters are estimated by the method we proposed, as shown within the dotted box in Fig. 1. Considering the time-invariant characteristics of the parameters, the state equation of the suspicious line parameters is established firstly. And the measurement equation is modified to the form that takes into account the suspicious parameters. Then the distribution network augmented state-space model is established by combining the state equation of the system state variables (voltage amplitude and phase angle of each bus), the parameter state equation and the modified measurement equation. Observing that the line parameters estimation is off-line, the augmented state-space model can be extended to the form under multiple measurement snapshots. The IAUKF consists of a UKF and a new fault-tolerance NSE [36]. The details of IAUKF are described in Section III. The NSE of IAUKF can accurately perceive the process noise statistical parameters and ensure the robustness of the algorithm during operation. Thus, the values of the suspicious line parameters can be estimated accurately by the augmented state estimation based on the IAUKF because the process noise statistical parameters of the system state variables and suspicious line parameters can be perceived by the NSE in the IAUKF.

III. The Improved Adaptive UKF

The UKF is a nonlinear filter that is widely used in the field of dynamic state estimation of power systems [31], [37]–[39]. But it can only guarantee superior performance if the process noise variance matrix $\mathbf{Q}_k$ and the measurement noise variance matrix $\mathbf{R}_k$ are accurately known. In the line parameters estimation problem, $\mathbf{R}_k$ can be obtained from the nameplate data of the measurement equipment and can be considered as known. However, $\mathbf{Q}_k$ is unknown and time-varying because the suspicious parameters are unknown and they are recursively corrected in each calculation. Therefore, the traditional UKF will be very difficult to estimate the accurate values of the suspicious parameters. To solve this issue, the IAUKF [36] is introduced in this paper with some modifications thus applicable to solve the line parameters estimation problem based on the augmented state estimation. A brief introduction of the modified IAUKF is given as follows:

Let a nonlinear system be shown in (1).

$$\begin{cases} x_k = f(x_{k-1}) + w_k \\ z_k = h(x_k) + v_k \end{cases} \tag{1}$$

where x_k and z_k are the n dimensional state vector and the m dimensional measurement vector at time step k, respectively; w_k and v_k are the process noise vector and measurement noise vector respectively where $w_k \sim N(0, \mathbf{Q}_k)$ and $v_k \sim N(0, \mathbf{R}_k)$; $f()$ is the state equation and $h()$ is the measurement equation.

The UKF selects a number of sigma points through the unscented transform (UT) to apply to the Kalman filter (KF) framework. It can be divided into three stages: prediction, correction and the process noise variance matrix estimation. The execution procedures are described in the following.

Stage 1. Prediction:

$$\begin{cases} X_{k-1}^{(0)} = \hat{x}_{k-1} \\ X_{k-1}^{(i)} = \hat{x}_{k-1} + \left(\sqrt{(n+\lambda)\,P_{k-1}}\right)_i, i = 1, 2, \ldots, n \\ X_{k-1}^{(i)} = \hat{x}_{k-1} - \left(\sqrt{(n+\lambda)\,P_{k-1}}\right)_i, i = n+1, \ldots 2n \end{cases} \tag{2}$$

$$\begin{cases} W_0^{(m)} = \frac{\lambda}{n+\lambda} \\ W_0^{(c)} = \frac{\lambda}{n+\lambda} + \left(1 - a^2 + \beta\right) \\ W_i^{(m)} = W_i^{(c)} = \frac{1}{2(n+\lambda)}, i = 1, 2, \ldots, 2n \end{cases} \tag{3}$$

where $\hat{x}_{k-1}$ and P_{k-1} are the state estimation result and the estimated error covariance matrix at time step $k-1$, respectively; The fine-tuning parameter $\lambda = a^2(n+\kappa) - n$ is used to control the point-to-mean distance; n is the state vector dimension; a is the proportional correction factor and the commonly used values is $10^{-4} \le a \le 1$ for Gaussian distribution; κ is the secondary sampling factor and its value is usually taken 0 or $3 - n$ [40]; β is the candidate parameter and $\beta = 2$ is optimal for the Gaussian distribution [41]; $(\sqrt{(n+\lambda)P_{k-1}})_i$ denotes the ith column of $\sqrt{(n+\lambda)P_{k-1}}$; $W_i^{(m)}$ and $W_i^{(c)}$ are the ith mean and variance calculation weights, respectively.

$$x_{k|k-1}^{(i)} = f(X_{k-1}^{(i)}), i = 0, 1, \ldots, 2n \tag{4}$$

$$\hat{x}_{k|k-1} = \sum_{i=0}^{2n} W_i^{(m)} x_{k|k-1}^{(i)} \tag{5}$$

$$P_{k|k-1} = \sum_{i=0}^{2n} W_i^{(c)} \left[x_{k|k-1}^{(i)} - \hat{x}_{k|k-1}\right] \times \left[x_{k|k-1}^{(i)} - \hat{x}_{k|k-1}\right]^{\mathrm{T}} + \mathbf{Q}_k \tag{6}$$

where $x_{k|k-1}^{(i)}$ is the sigma point propagated through the state equation; $\hat{x}_{k|k-1}$ is the state prediction value obtained by propagation; $P_{k|k-1}$ is the prediction covariance matrix of the state variable.

Stage 2. Correction:

$$\begin{cases} X_{k|k-1}^{(0)} = \hat{x}_{k|k-1} \\ X_{k|k-1}^{(i)} = \hat{x}_{k|k-1} + \left(\sqrt{(n+\lambda)\,P_{k|k-1}}\right)_i, i = 1, 2, \ldots, n \\ X_{k|k-1}^{(i)} = \hat{x}_{k|k-1} - \left(\sqrt{(n+\lambda)\,P_{k|k-1}}\right)_i, i = n+1, \ldots, 2n \end{cases} \tag{7}$$

$$Z_{k|k-1}^{(i)} = h(X_{k|k-1}^{(i)}), i = 1 = 0, 1, \ldots, 2n \tag{8}$$

$$\hat{z}_{k|k-1} = \sum_{i=0}^{2n} W_i^{(m)} Z_{k|k-1}^{(i)} \tag{9}$$

$$P_{zz,k|k-1} = \sum_{i=0}^{2n} W_i^{(c)} \left[Z_{k|k-1}^{(i)} - \hat{z}_{k|k-1}\right] \times \left[Z_{k|k-1}^{(i)} - \hat{z}_{k|k-1}\right]^{\mathrm{T}} + \mathbf{R}_k \tag{10}$$

$$P_{xz,k|k-1} = \sum_{i=0}^{2n} W_i^{(c)} \left[X_{k|k-1}^{(i)} - \hat{x}_{k|k-1}\right] \times \left[Z_{k|k-1}^{(i)} - \hat{z}_{k|k-1}\right]^{\mathrm{T}} \tag{11}$$

where $Z_{k|k-1}^{(i)}$ is the sigma point propagated through the measurement equation at time step k; $\hat{z}_{k|k-1}$ is the measured prediction value obtained by the propagation; $P_{zz,k|k-1}$ and $P_{xz,k|k-1}$ are the covariance matrix and the cross-covariance matrix of the predicted measurement, respectively.

$$K_k = P_{xz,k|k-1} P_{zz,k|k-1}^{-1}. \tag{12}$$

$$\hat{x}_k = \hat{x}_{k|k-1} + K_k \left(z_k - \hat{z}_{k|k-1}\right). \tag{13}$$

$$P_k = P_{k|k-1} - K_k P_{zz,k|k-1} K_k^{\mathrm{T}}. \tag{14}$$

The estimated state vector $\hat{x}_k$ is obtained and the covariance matrix P_k is updated after the stage of correction.

Stage 3. The process noise variance matrix estimation:

To perceive $\mathbf{Q}_k$ in the process of the UKF, it is necessary to estimate its value by embedding the NSE [36] into the UKF.

$$\varepsilon_k = z_k - \hat{z}_{k|k-1} \tag{15}$$

$$d_k = (1-b) / \left(1 - b^{k+1}\right) \tag{16}$$

$$\mathbf{Q}_{k+1} = (1-d_k)Q_k + d_k \Bigg[K_k \varepsilon_k \varepsilon_k^{\mathrm{T}} K_k^{\mathrm{T}} + P_k - \sum_{i=0}^{2n} W_i^{(c)} \left(X_{k|k-1}^{(i)} - \hat{x}_{k|k-1} \right) \left(X_{k|k-1}^{(i)} - \hat{x}_{k|k-1} \right)^{\mathrm{T}} \Bigg] \tag{17}$$

$$\mathbf{Q}_{k+1} = \begin{cases} \mathbf{Q}_{k+1}, \text{if } \mathbf{Q}_{k+1} \text{ is nonnegative definite} \\ (1-d_k)\, \mathbf{Q}_k + d_k [diag\left(K_k \varepsilon_k \varepsilon_k^{\mathrm{T}} K_k^{\mathrm{T}}\right) \\ + K_k P_{zz,k|k-1} K_k^{\mathrm{T}}], \text{otherwise} \end{cases} \tag{18}$$

where ε_k is the residual between the system measurement and the predicted measurement at time step k; b is the forgetting factor and $0.95 \leq b \leq 0.995$, which is set to be 0.96 in this paper; $diag()$ is the function returning a diagonal matrix of the same dimension as the operation matrix that is made up of the diagonal elements of the operated matrix. $\mathbf{Q}_{k+1}$ is recalculated by the biased NSE in (18) if its value calculated by the unbiased NSE in (17) loses the nonnegative definiteness.

IV. Proposed Augmented State-Space Model

To estimate the suspicious parameters by the augmented state estimation, the distribution network augmented state-space model needs to be established. The state equation of suspicious line parameters can be established based on their time-invariant characteristics. The measurement equation is modified with the consideration of the suspicious parameters. The developed augmented state-space model for dynamic state estimation based on the IAUKF is developed by combining the state equation of the system state variables (voltage amplitude and phase angle of each bus), the parameter state equation and the modified measurement equation. Since the line parameters are constant over a certain period and can be estimated off-line, the augmented state-space model can be extended to the form under multiple measurement snapshots to avoid the failure of estimation due to the insufficient measurement redundancy.

A. Distribution Network State-Space Model

The distribution network state variable $x_k = [V_i, \delta_i]^{\mathrm{T}}$ is the voltage amplitude and phase angle of each bus at time step k. Its state equation is established by Holt's dual exponential smoothing method. The distribution network state equation $f()$ can be expressed as (19).

$$\begin{cases} x_{k|k-1} = S_{k-1} + b_{k-1} \\ S_{k-1} = \alpha_{\mathrm{H}} x_{k-1} + (1-\alpha_{\mathrm{H}}) x_{k-1|k-2} \\ b_{k-1} = \beta_{\mathrm{H}}(S_{k-1} - S_{k-2}) + (1-\beta_{\mathrm{H}}) b_{k-2} \end{cases} \tag{19}$$

where x_{k-1} represents the state value of the distribution network at time step $k-1$; $x_{k|k-1}$ indicates the state prediction value at time step k obtained by the state equation; $S_{k\text{-}1}$ and $b_{k\text{-}1}$ are the horizontal and vertical components, respectively; α_{H} and β_{H} are called the smoothing parameter and their value are usually taken in $[0, 1]$. In this work, the smoothing parameters of $\alpha_{\mathrm{H}} = 0.8$ and $\beta_{\mathrm{H}} = 0.5$ are adopted, as suggested in [42].

Based on the measurement type of SCADA and PMU, the measurement vector is composed as (20) in the distribution network. The voltage phasor measurement can only be obtained at the buses configured with the PMU.

$$z_k = \left[V_i, P_i, Q_i, P_{ij}, Q_{ij}, \delta_i^{(PMU)} \right]^{\mathrm{T}} \tag{20}$$

where V_i and $\delta_i^{(PMU)}$ are the voltage amplitude and phase angle of the bus i, respectively; P_i and Q_i are the injected active and reactive power of the bus, respectively; P_{ij} and Q_{ij} are the active and reactive power of the branch $i-j$.

Associating with the measurement types in z_k, the measurement equation $h()$ is as follows:

$$\begin{cases} V_i = V \\ P_i = V_i \sum\limits_j V_j (G_{ij} \cos\delta_{ij} + B_{ij} \sin\delta_{ij}) \\ Q_i = V_i \sum\limits_j V_j (G_{ij} \sin\delta_{ij} - B_{ij} \cos\delta_{ij}) \\ P_{ij} = V_i^2 g_{ij} - V_i V_j g_{ij} \cos\delta_{ij} - V_i V_j b_{ij} \sin\delta_{ij} \\ Q_{ij} = -V_i^2 b_{ij} - V_i V_j g_{ij} \sin\delta_{ij} + V_i V_j b_{ij} \cos\delta_{ij} \\ \delta_i^{(PMU)} = \delta_i \end{cases} \tag{21}$$

where G_{ij} and B_{ij} are the real and imaginary parts of the element of the ith row and jth column of the node admittance matrix, respectively; g_{ij} and b_{ij} are the conductance and susceptance of the branch $i-j$, respectively; $\delta_{ij} = \delta_i - \delta_j$.

Combining the state equation with the measurement equation, the state-space model can be established as (22).

$$\begin{cases} x_k = f(x_{k-1}) + w_{x|k} \\ z_k = h(x_k) + v_k \end{cases} \tag{22}$$

where $w_{x|_k}$ is the process noise vector of the state variable at time step k and $w_{x|k} \sim N(0, \mathbf{Q}_{x|k})$; v_k is the measurement noise vector and $v_k \sim N(0, \mathbf{R}_k)$; $\mathbf{R}_k$ can be obtained by the nameplate data of the measurement equipment as mentioned before; $\mathbf{Q}_{x|k}$ changes with the fluctuation of the load, therefore it is unknown and time-varying. Hence, it is necessary to be estimated by the NSE of IAUKF.

B. Distribution Network Augmented State-Space Model

The suspicious parameters are set as unknown parameter variables. The augmented state vector is constituted by combining the unknown parameter state variables and the system state variables as (23)∼(25).

$$\bar{x}_k = [x_k p_k]^{\mathrm{T}} \tag{23}$$

$$x_k = [V_i, \delta_i]^{\mathrm{T}} \tag{24}$$

$$p_k = [r_1, x_1, r_2, x_2, \ldots, r_p, x_p]^{\mathrm{T}} \tag{25}$$

where the augmented state vector $\bar{x}_k$ includes two parts: the system state vector x_k and the parameter state vector p_k; p_k consists of $2p$ dimensional resistance and reactance parameters when the number of suspicious lines is p.

Similar to the state transition equation of synchronous machine [32], [34], the state equation of line parameters can be given as (26). The intuition behind (26) is that the line parameters of the time step k and $k-1$ should be equal when the parameter values are accurately estimated.

$$p_k = p_{k-1} + w_{p|k} \tag{26}$$

where $w_{p|k}$ is the process noise vector of the parameter variables at time step k, which is assumed to be Gaussian white noise to be applicable to the framework of IAUKF, i.e., $w_{p|k} \sim N(0, \mathbf{Q}_{p|k})$. The parameters are uncorrelated with each other.

The augmented state equation can be established by combining the system state equation (19) with the parameter state equation (26), as shown in (27).

$$\bar{x}_k = \begin{bmatrix} f(x_{k-1}) \\ p_{k-1} \end{bmatrix} + \begin{bmatrix} w_{x|k} \\ w_{p|k} \end{bmatrix}. \tag{27}$$

The process noise variance matrix of the augmented state equation is a block diagonal matrix as shown in (28) since the state vector of the system and the parameter vector are uncorrelated.

$$\mathbf{Q}_k = \begin{bmatrix} \mathbf{Q}_{x|k} & 0 \\ 0 & \mathbf{Q}_{p|k} \end{bmatrix}. \tag{28}$$

The measurement equation reflects the relationship between the measurement and the state vector, and its construction requires line parameters. When the suspicious parameters are considered as unknown parameter variables like system state variables, the measurement equation need to be modified to the form considering parameter variables as (29).

$$z_k = h(x_k, p_k) + v_k. \tag{29}$$

Through combining (27) and (29), the augmented state-space model can be obtained as follows:

$$\begin{cases} \bar{x}_k = \begin{bmatrix} f(x_{k-1}) \\ p_{k-1} \end{bmatrix} + \begin{bmatrix} w_{x|k} \\ w_{p|k} \end{bmatrix} \\ z_k = h(x_k, p_k) + v_k \end{cases}. \tag{30}$$

The process noise of the parameter variables reflects the deviation between the true parameter values and the current parameter estimation values. Since the true parameter values are unknown, and the measurement will correct the parameter estimation values at each time step, this deviation is unknown and time-varying. Hence, the process noise variance matrix $\mathbf{Q}_{p|k}$ of the parameter variables cannot be assumed constant and requires estimation during the parameter estimation.

C. Distribution Network Augmented State-Space Model Under Multiple Measurement Snapshots

The line parameters estimation can be implemented off-line, and the line parameters remain constant over a certain period. In addition, as shown in (31), the measurement redundancy can be effectively improved by applying multiple measurement snapshots data. Therefore, the augmented state-space model can be extended to the form under multiple measurement snapshots to avoid the failure of estimation caused by insufficient measurement redundancy.

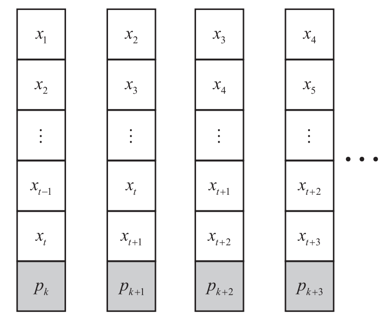

Fig. 2. The structure of the augmented state vector.

$$\frac{mt}{nt + n_p} = \frac{m}{n + n_p/t} > \frac{m}{n + n_p} \tag{31}$$

where n_p, t, m and n are the dimension of the unknown parameters, the number of the used multiple measurement snapshots, the measurement and system state vector dimension, respectively.

The state and measurement vector need to be reconstructed when using data under multiple measurement snapshots. Herein, the augmented state vector $\bar{X}_k$ is the combination of the system state vector of multiple time steps and the unknown parameter state vector, as shown in (32). Also, the measurement vector Z_k also needs to be reconstructed correspondingly as (34).

$$\bar{X}_k = [X_k p_k]^{\mathrm{T}} \tag{32}$$

$$X_k = [x_1, x_2, \ldots, x_t] \tag{33}$$

$$Z_k = [z_1, z_2, \ldots, z_t]^{\mathrm{T}} \tag{34}$$

where x_t and z_t are the system state and measurement vector at time step t, respectively.

The augmented state vector at each step is shown in Fig. 2. It can be seen from Fig. 2 that the part of the system state vector under multiple measurement snapshots between two steps are still adjacent time steps at the corresponding positions. Hence, the state equation under multiple measurement snapshots can be obtained by expanding (27) as shown in (35).

$$\bar{X}_k = \begin{bmatrix} f(X_{k-1}) \\ p_{k-1} \end{bmatrix} + \begin{bmatrix} w_{X|k} \\ w_{p|k} \end{bmatrix}. \tag{35}$$

Also, the measurement equation under multiple measurement snapshots can be obtained by expanding (29) as follows:

$$Z_k = \begin{bmatrix} z_1 \\ z_2 \\ \vdots \\ z_t \end{bmatrix} = \begin{bmatrix} h(x_1, p_k) \\ h(x_2, p_k) \\ \vdots \\ h(x_t, p_k) \end{bmatrix} + \begin{bmatrix} v_{1|k} \\ v_{2|k} \\ \vdots \\ v_{t|k} \end{bmatrix}. \tag{36}$$

Correspondingly, the process and measurement noise variance matrix are shown in (37) and (38), respectively.

$$\mathbf{Q}_k = \operatorname{diag}\left(\mathbf{Q}_{x|1}, \mathbf{Q}_{x|2}, \ldots, \mathbf{Q}_{x|t}, \mathbf{Q}_{p|k}\right). \tag{37}$$

TABLE I
THE CONFIGURATION PARAMETERS OF MEASUREMENT

Measurement type	Bus configuration
SCADA	1,2,4,5,7,8,10,12,13,15,16,18, 20,21,23,25,27,28,30,31,33
PMU	3,6,9,11,14,17,19,22,24,26,29,32

$$\mathbf{R}_k = \mathrm{diag}\left(\mathbf{R}_1, \mathbf{R}_2, \ldots, \mathbf{R}_t\right). \tag{38}$$

V. SIMULATION EXPERIMENTS AND NUMERICAL RESULTS

In this work, the IEEE 33-bus system [43] and the 118-bus system [44] constructed in MATPOWER [45] are adopted to verify the effectiveness of the proposed method. To have more realistic case studies, the measurement data used in the simulation are obtained by adding Gaussian noise into the results of power flow [12]. And the power flow is calculated by MATPOWER. The standard deviation of SCADA measurement is set to 0.02. The standard deviations of PMU voltage amplitude and phase angle are set to be 0.005 and 0.002, respectively. The parameters required for the UKF are: $a = 0.001$, $\kappa = 0$ and $\beta = 2$. And the initial $\mathbf{Q}_k$ is set to be $10^{-6}\mathbf{I}$ [32], [35] which will be adaptive during the parameter estimation. Because the true values of suspicious parameters are unknown, the initial values are set to be a small value (e.g., 0.01 or 0.02). The difference between the two adjacent steps estimation results will become small when the results tend to converge. To determine the convergence step, the convergence criterion is established as (39).

$$|p_k - p_{k-1}| \leq \delta \tag{39}$$

where δ is the accuracy requirement which is set to be 0.001 in this paper.

When both the resistance and reactance parameters satisfy the convergence criteria, the average values of all parameter estimation results after convergence are obtained as the final estimation results, as shown in (40).

$$\hat{p} = \frac{\sum_{k=n}^{N} p_k}{L} \tag{40}$$

where n is the step of convergence; N is the total number of steps and $L = N - n + 1$.

A. Simulations on the IEEE 33-Bus System

The effectiveness of the proposed method is first verified in the case that there are suspicious line parameters of a single branch of the IEEE 33-bus system. The measurement configuration is shown in Table I. It is assumed that the parameters of branch 3–4 are unknown. Thus, its resistance and reactance are treated as state variables and are augmented into the state vector. After the augmented vector is estimated by the IAUKF for 200-time steps under single measurement snapshot, the result curves of the parameters are shown in Fig. 3. It can be seen from Fig. 3 that both the resistance and reactance of the branch converge to straight lines after estimation in a certain number of time steps. To improve the estimation accuracy, the final estimation

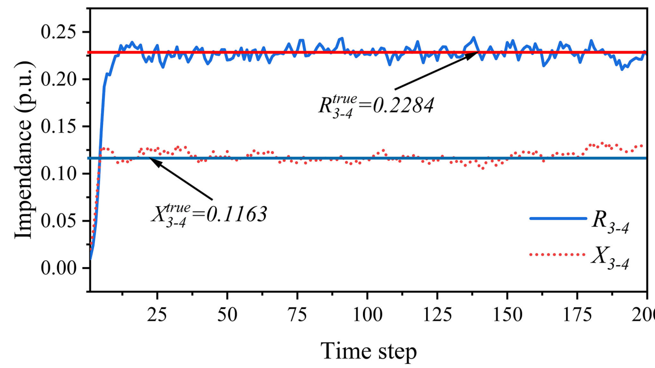

Fig. 3. Estimation of branch 3-4 under single measurement snapshot.

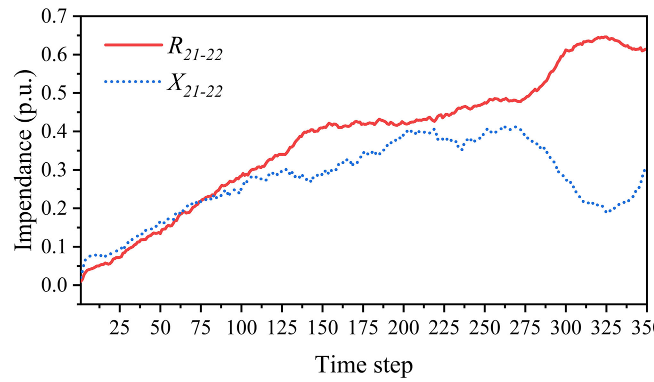

Fig. 4. Estimation results of branch 21-22 under single measurement snapshot.

results are obtained by (39) and (40). The relative errors of the final results of resistance and reactance are 0.18% and 1.55%, respectively. Both the resistance and reactance can be accurately estimated.

To further validate the effectiveness of the proposed method for the parameters of each branch under single measurement snapshot, the parameters of other 31 branches are set as unknown and estimated by the IAUKF respectively. After a certain number of time steps of performing, all parameters, except the parameters of the four end branches (17–18, 21–22, 24–25 and 32–33) can converge to straight lines and obtain well-estimated results.

The estimation results of the four end branches can't converge under single measurement snapshot, such as the estimation results of the parameters of the branch 21–22 shown in Fig. 4. Even though 350 time-steps have been recursively estimated, they still do not converge. This is because of the insufficient measurement redundancy for end branches when estimation. Therefore, to increase the measurement redundancy and enable the estimation of the parameters of end branches, the augmented state-space model under multiple measurement snapshots is adopted. The number of the measurement snapshots is set to be 5, and the estimation results of branch 21-22 are shown in Fig. 5. The parameters of the branch converge to straight lines after estimation in a certain number of steps by increasing the measurement redundancy. The relative errors of the final results

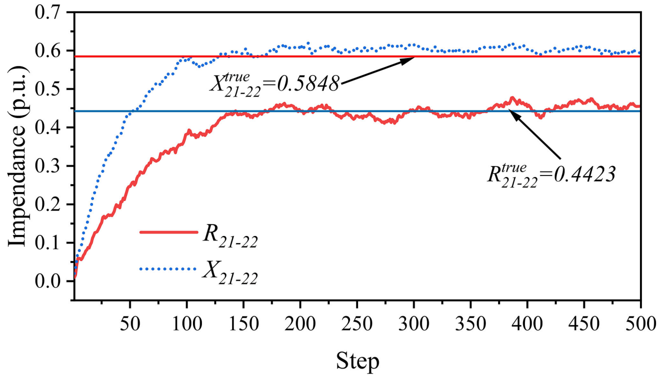

Fig. 5. Estimation of branch 21-22 under multiple measurement snapshots.

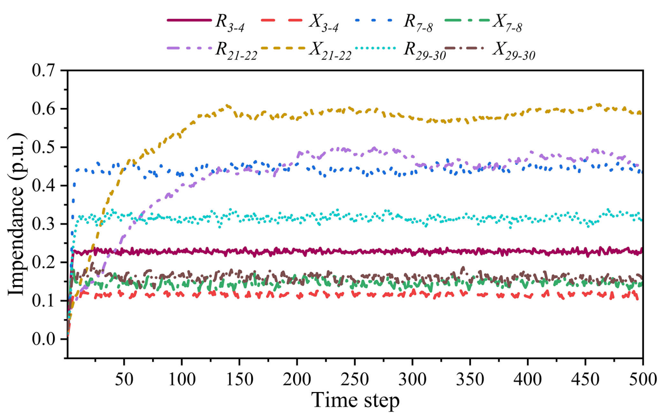

Fig. 6. Estimation of four branches under multiple measurement snapshots.

TABLE II
ESTIMATION RESULTS OF FOUR BRANCHES

Branch (bus # - bus #)		3-4	7-8	21-22	29-30
Resistance	True value (p.u)	0.2284	0.4439	0.4423	0.3166
	Estimated value (p.u)	0.2281	0.4436	0.4446	0.3157
	Estimation error (%)	0.13%	0.07%	0.52%	0.28%
Reactance	True value (p.u)	0.1163	0.1467	0.5848	0.1613
	Estimated value (p.u)	0.1162	0.1463	0.5729	0.1601
	Estimation error (%)	0.09%	0.27%	2.03%	0.74%

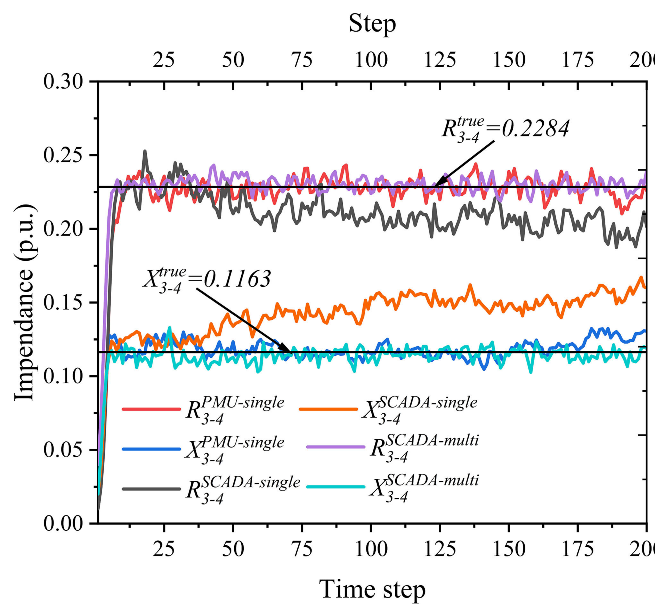

Fig. 7. The comparison of the parameter estimation results of branch 3-4 with and without configuration of PMU.

under multiple measurement snapshots are 0.36% and 2.96%. The results show that the augmented state-space model under multiple measurement snapshots can effectively improve the measurement redundancy and avoid the failure of estimation caused by insufficient measurement redundancy. Thus, when the parameters of multi-branch are suspicious, the accurate estimation results can be obtained by using the model under multiple measurement snapshots.

It is assumed that the parameters of 4 branches including the end branches are suspicious to analyze the estimation performance when the parameters of multiple branches are unknown. The 8 unknown parameters are augmented into the state vector for the model under multiple measurement snapshots. And, the number of the measurement snapshots still is 5. The estimation results are shown in Fig. 6. As can be seen from Fig. 6, the 8 parameters can converge to estimated values. The final estimation values are shown in Table II. According to the table, the relative errors of resistance and reactance of estimated values for branch 3–4 are 0.13% and 0.09% which are more accurate than those under single snapshot (noting that the relative errors of resistance and reactance are 0.18% and 1.55%, respectively.). This indicates that the improvement of measurement redundancy not only guarantees the accurate estimation of the end branch parameters but also can obtain the more accurate estimated values of other branches. In summary, the proposed method in this paper can obtain accurate estimated values when both single-branch and multi-branch parameters are unknown.

The PMU configured in the distribution network can provide high precision measurements, which helps to improve the accuracy of parameter estimation. Fig. 7 and Fig. 8 show the comparison of the parameter estimation results with and without configuration of μPMU. According to the Fig. 7, the accuracy of the estimation results $R_{3-4}^{PMU-single}$ and $X_{3-4}^{PMU-single}$ under single measurement snapshot with the PMU is resembled as the results $R_{3-4}^{SCADA-multi}$ and $X_{3-4}^{SCADA-multi}$ under multiple measurement snapshots without the PMU while the results $R_{3-4}^{SCADA-single}$ and $X_{3-4}^{SCADA-single}$ have large errors. It indicates not only that the PMU can improve the estimation accuracy, but also that the improvement of the redundancy of the measurement can improve the estimation accuracy. Moreover, Fig. 8 indicates that the error of the results R_{21-22}^{SCADA} and X_{21-22}^{SCADA} without the PMU under multiple measurement snapshots is obviously higher than the results R_{21-22}^{PMU} and X_{21-22}^{PMU} with the PMU under multiple measurement snapshots. This demonstrates the effectiveness of PMU in improving estimation accuracy

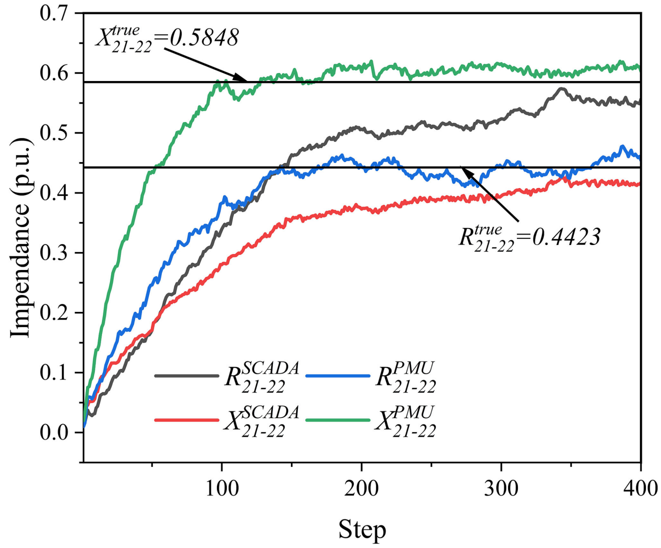

Fig. 8. The comparison of the parameter estimation results of branch 21-22 with and without configuration of PMU.

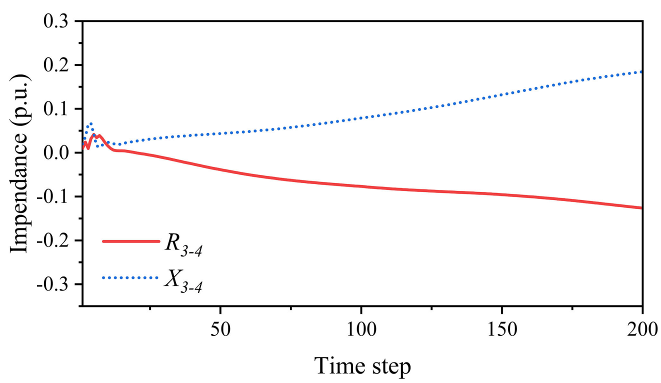

Fig. 9. $\mathbf{Q}_k$ keeps a constant under single measurement snapshot.

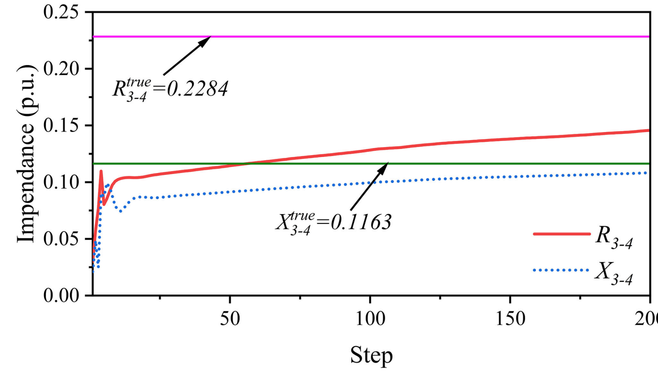

Fig. 10. $\mathbf{Q}_k$ keeps a constant under multiple measurement snapshots.

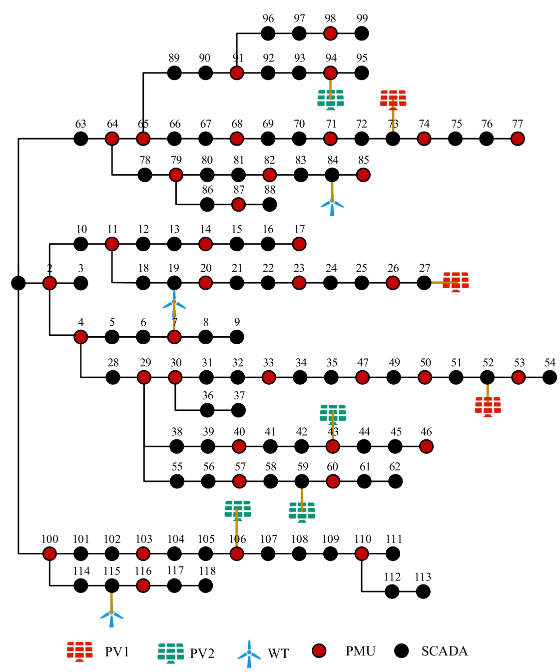

Fig. 11. The topology of the 118-bus system.

and the necessity of configuring μPMU in a large distribution network.

In order to test the necessity of perceiving $\mathbf{Q}_k$ in the process of UKF, the UKF that keeps $\mathbf{Q}_k$ as a constant is performed to estimate the line parameters of branch 3-4 under single and multiple measurement snapshots. As evident from Fig. 9 and Fig. 10, the estimated results fail to converge to the true values in the two cases. In contrast, the estimation results of the method proposed in this paper can quickly converge to the true values under single measurement snapshot as shown in Fig. 3.

B. Simulations on the 118-Bus System

To further validate the performance of the proposed method in this paper, the 118-bus system with DGs is adopted. The total load of the system is 22709.7kW+j17041.1kVar. The penetration rate of DGs is set to be 20%. And, the 118-bus system topology, measurement configuration and DG configuration are shown Fig. 11. The rated capacities of PV1, PV2 and WT are 400kW+j132kVar, 600kW+j196kVar and 300kW+j90kVar, respectively. The conclusion obtained from the simulation results of the 118-bus system with DGs is consistent with those in the IEEE 33-bus system. For instance, it can be seen from Fig. 12 that the result curves of branch 64-78 under single measurement snapshot can converge to estimated values. However, the result curves of end branch 16-17 under single measurement snapshot can't converge as shown in Fig. 13. Consistent with the IEEE 33-bus system, the model under multiple measurement snapshots (noting that the number of the snapshots is set to 10) can give accurate estimated values of the parameters of branch 16-17 according to Fig. 14.

The parameters of 21 randomly selected branches are considered to be unknown. These 42 parameters are augmented to the state vector under multiple measurement snapshots and estimated simultaneously. The relative errors of the estimated results for all branch resistances and reactances are shown in Fig. 15. All parameters can be estimated well. The mean relative errors of R and X are 0.18% and 0.27%, respectively. These

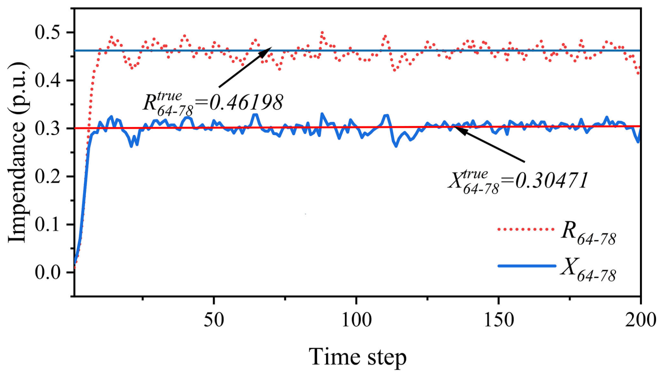

Fig. 12. Estimation of branch 64-78 under single measurement snapshot.

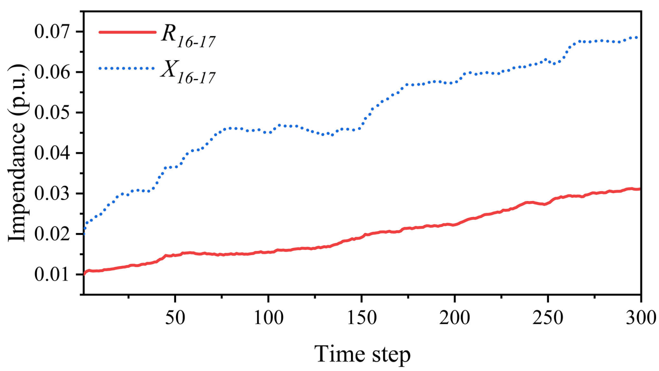

Fig. 13. Estimation of branch 16-17 under single measurement snapshot.

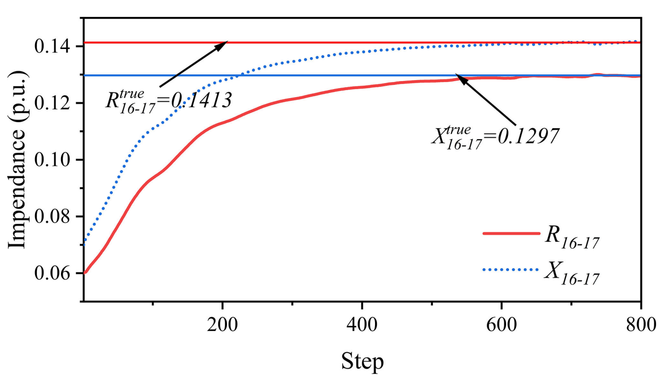

Fig. 14. Estimation of branch 16-17 under multiple measurement snapshots.

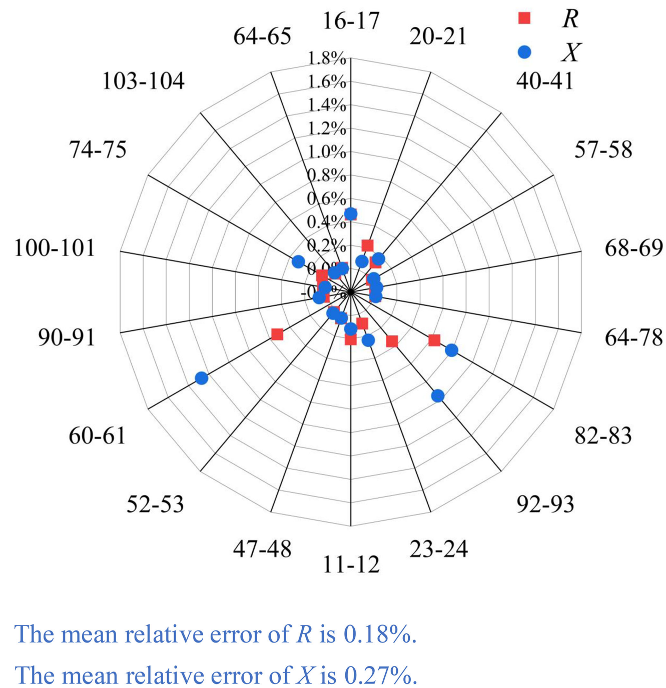

Fig. 15. The relative errors of estimated results of all parameters.

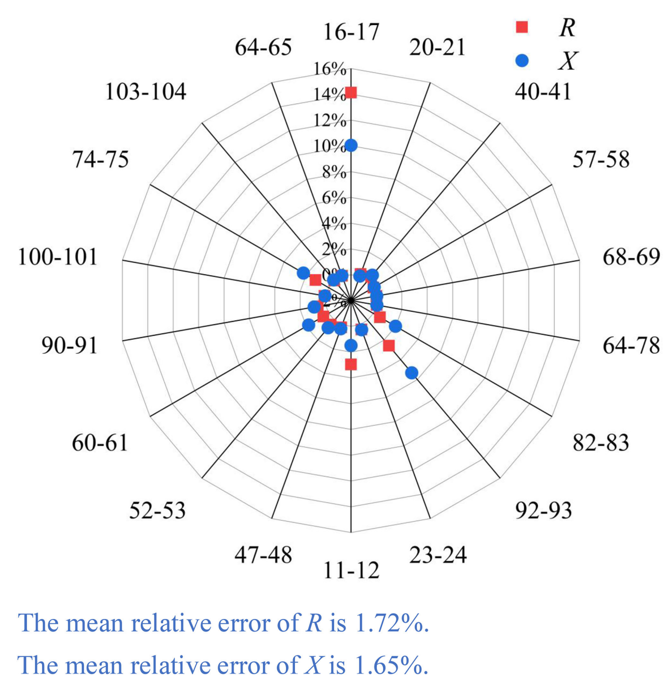

Fig. 16. The relative errors of estimated results of all parameters under bad data.

results show that the method proposed in this paper performs well in the case of large systems with DGs and with unknown multi-branch parameters.

The model under multiple measurement snapshots effectively improves the measurement redundancy, which will enhance the robustness of the proposed method for bad data. Bad data mainly include erroneous data with large errors and missing data due to communication failures. The estimation performance of the parameters of 21 branches is evaluated by considering the case of 10% of measurements are bad data at each time step, of which 5% are missing data and 5% are erroneous data. The erroneous data is obtained by adding 3 times of Gaussian noise into the results of power flow. The estimated results are shown in Fig. 16. The estimation results of the parameters of all branches yield good performance, i.e. the mean relative errors of R and X are 1.72% and 1.65%, respectively. The branch 16–17 is with higher relative errors that are still considered acceptable. The estimated results demonstrate the robustness of the proposed model under multiple measurement snapshots.

VI. Conclusion

This paper present an recursive estimation method of erroneous distribution line parameters based on augmented state estimation. The parameter state equation is firstly formulated by the time-invariant characteristics of parameters. Afterward, the augmented state-space models under single and multiple measurement snapshots are established separately by combining the parameter state equation with state-space model of the distribution network. The model under multiple measurement snapshots can improve the estimation accuracy effectively and avoid the failure of estimation due to insufficient measurement redundancy. In order to perceive the process noise statistical parameters during the parameter estimation, the augmented state estimation based on the IAUKF is developed. The proposed approach is implemented and extensively validated. The numerical simulations on the IEEE 33-bus system indicate that the proposed method can accurately estimate the suspicious parameters both in the cases with single-branch and multi-branch errors, even if the end branches are included. Also, the numerical simulations on the 118-bus system with DGs demonstrate the scalability and the robustness for bad data of the proposed algorithm.

References

[1] F. R. Badal, P. Das, S. K. Sarker, and S. K. Das, "A survey on control issues in renewable energy integration and microgrid," *Protection Control Modern Power Syst.*, vol. 4, no. 8, pp. 1–27, 2019.

[2] A. P. S. Meliopoulos, E. Polymeneas, Z. Tan, R. Huang, and D. Zhao, "Advanced distribution management system," *IEEE Trans. Smart Grid*, vol. 4, no. 4, pp. 2109–2117, Dec. 2013.

[3] A. Primadianto and C. Lu, "A review on distribution system state estimation," *IEEE Trans. Power Syst.*, vol. 32, no. 5, pp. 3875–3883, Sep. 2017.

[4] A. Tajer, S. Sihag, and K. Alnajjar, "Non-linear state recovery in power system under bad data and cyber attacks," *J. Modern Power Syst. Clean Energy*, vol. 7, no. 5, pp. 1071–1080, 2019.

[5] A. Abur and A. G. Exposito, *Power System State Estimation: Theory and Implementation*. Boca Raton, FL, USA: CRC Press, 2004.

[6] X. Dong, C. Kang, H. Sun, and N. Zhang, "Analysis of power transfer limit considering thermal balance of overhead conductor," *IET Gener., Transmiss. Distrib.*, vol. 9, no. 14, pp. 2007–2013, 2015.

[7] Y. Wang, W. Xu, and J. Shen, "Online tracking of transmission-line parameters using SCADA data," *IEEE Trans. Power Del.*, vol. 31, no. 2, pp. 674–682, Apr. 2016.

[8] G. Kusic and D. Garrison, "Measurement of transmission line parameters from SCADA data," in *Proc. IEEE PES Power Syst. Conf. Expo.*, 2004, pp. 440–445, doi: 10.1109/PSCE.2004.1397479.

[9] J. Zhang, Y. Wang, Y. Weng, and N. Zhang, "Topology identification and line parameter estimation for non-PMU distribution network: A numerical method," *IEEE Trans. Smart Grid*, vol. 11, no. 5, pp. 4440–4453, Sep. 2020.

[10] M. R. M. Castillo, N. G. Bretas, and J. B. A. London, "Improved branch parameter errors detection, identification and correction," in *Proc. PES TD*, 2012, pp. 1–7, doi: 10.1109/TDC.2012.6281590.

[11] M. R. M. Castillo, J. B. A. London, and N. G. Bretas, "Identification and estimation of power system branch parameter error," in *IEEE Power Energy Soc. Gen. Meeting*, 2009, pp. 1–8, doi: 10.1109/PES.2009.5275219.

[12] M. Asprou and E. Kyriakides, "Identification and estimation of erroneous transmission line parameters using PMU measurements," *IEEE Trans. Power Del.*, vol. 32, no. 6, pp. 2510–2519, Dec. 2017.

[13] S. Kurokawa, J. Pissolato, M. C. Tavares, C. M. Portela, and A. J. Prado, "A new procedure to derive transmission-line parameters: Applications and restrictions," *IEEE Trans. Power Del.*, vol. 21, no. 1, pp. 492–498, Jan. 2006.

[14] W. E. Liu and L. Swee-Lian, "Parameter error identification and estimation in power system state estimation," *IEEE Trans. Power Syst.*, vol. 10, no. 1, pp. 200–209, Feb. 1995.

[15] M. Asprou and E. Kyriakides, "Estimation of line parameters using the hybrid state estimator," in *Proc. IEEE Grenoble Conf.*, 2013, pp. 1–6, doi: 10.1109/PTC.2013.6652160.

[16] Y. Lin and A. Abur, "Enhancing network parameter error detection and correction via multiple measurement scans," *IEEE Trans. Power Syst.*, vol. 32, no. 3, pp. 2417–2425, May 2017.

[17] J. B. A. London, L. Mili, and N. G. Bretas, "An observability analysis method for a combined parameter and state estimation of a power system," in *Proc. Int. Conf. Probabilistic Methods Appl. Power Syst.*, 2004, pp. 594–599, doi: 10.1109/PTC.2013.6652160.

[18] O. Alsac, N. Vempati, B. Stott, and A. Monticelli, "Generalized state estimation," *IEEE Trans. Power Syst.*, vol. 13, no. 3, pp. 1069–1075, Aug. 1998.

[19] M. R. Castillo, J. B. London, N. G. Bretas, S. Lefebvre, J. Prévost, and B. Lambert, "Offline detection, identification, and correction of branch parameter errors based on several measurement snapshots," *IEEE Trans. Power Syst.*, vol. 26, no. 2, pp. 870–877, May 2010.

[20] S. Gajare, A. K. Pradhan, and V. Terzija, "A method for accurate parameter estimation of series compensated transmission lines using synchronized data," *IEEE Trans. Power Syst.*, vol. 32, no. 6, pp. 4843–4850, Nov. 2017.

[21] K. V. Khandeparkar, S. A. Soman, and G. Gajjar, "Detection and correction of systematic errors in instrument transformers along with line parameter estimation using PMU data," *IEEE Trans. Power Syst.*, vol. 32, no. 4, pp. 3089–3098, Jul. 2017.

[22] D. Ritzmann, P. S. Wright, W. Holderbaum, and B. Potter, "A method for accurate transmission line impedance parameter estimation," *IEEE Trans. Instrum. Meas.*, vol. 65, no. 10, pp. 2204–2213, Oct. 2016.

[23] Y. Hou, T. Fang, F. Shi, and H. Zhang, "Parameter estimation method of distribution network based on PMU measurement data," in *Proc. 5th Asia Conf. Power Elect. Eng.*, 2020, pp. 1620–1625, doi: 10.1109/ACPEE48638.2020.9136244.

[24] E. Y. Song, G. J. FitzPatrick, and K. B. Lee, "Smart sensors and standard-based interoperability in smart grids," *IEEE Sensors J.*, vol. 17, no. 23, pp. 7723–7730, Dec. 2017.

[25] Y. Liu, L. Wu, and J. Li, "D-PMU based applications for emerging active distribution systems: A review," *Electric Power Syst. Res.*, vol. 179, 2020, Art. no. 106063.

[26] J. Yu, Y. Weng, and R. Rajagopal, "PaToPa: A data-driven parameter and topology joint estimation framework in distribution grids," *IEEE Trans. Power Syst.*, vol. 33, no. 4, pp. 4335–4347, May 2018.

[27] R. Dutta, V. S. Patel, S. Chakrabarti, A. Sharma, R. K. Das, and S. Mondal, "Parameter estimation of distribution lines using SCADA measurements," *IEEE Trans. Instrum. Meas.*, vol. 70, pp. 1–11, 2021. Art. no. 9000411, doi: 10.1109/TIM.2020.3026116.

[28] P. A. Pegoraro, K. Brady, P. Castello, C. Muscas, and A. v. Meier, "Compensation of systematic measurement errors in a PMU-Based monitoring system for electric distribution grids," *IEEE Trans. Instrum. Meas.*, vol. 68, no. 10, pp. 3871–3882, Oct. 2019.

[29] P. A. Pegoraro, K. Brady, P. Castello, C. Muscas, and A. v. Meier, "Line impedance estimation based on synchrophasor measurements for power distribution systems," *IEEE Trans. Instrum. Meas.*, vol. 68, no. 4, pp. 1002–1013, Apr. 2019.

[30] J. Sun, M. Xia, and Q. Chen, "A classification identification method based on phasor measurement for distribution line parameter identification under insufficient measurements conditions," *IEEE Access*, vol. 7, pp. 158732–158743, 2019.

[31] J. Zhao and L. Mili, "Robust unscented Kalman filter for power system dynamic state estimation with unknown noise statistics," *IEEE Trans. Smart Grid*, vol. 10, no. 2, pp. 1215–1224, Mar. 2019.

[32] G. Valverde, E. Kyriakides, G. T. Heydt, and V. Terzija, "Nonlinear estimation of synchronous machine parameters using operating data," *IEEE Trans. Energy Convers.*, vol. 26, no. 3, pp. 831–839, Sep. 2011.

[33] A. Rouhani and A. Abur, "Constrained iterated unscented Kalman filter for dynamic state and parameter estimation," *IEEE Trans. Power Syst.*, vol. 33, no. 3, pp. 2404–2414, May 2018.

[34] M. Huang, W. Li, and W. Yan, "Estimating parameters of synchronous generators using square-root unscented Kalman filter," *Electric Power Syst. Res.*, vol. 80, no. 9, pp. 1137–1144, 2010.

[35] A. Rouhani and A. Abur, "Real-time dynamic parameter estimation for an exponential dynamic load model," *IEEE Trans. Smart Grid*, vol. 7, no. 3, pp. 1530–1536, May 2016.

[36] X. Fang, L. Nan, Z. Jiang, and L. Chen, "Robust node position estimation algorithms for wireless sensor networks based on improved adaptive Kalman filters," *Comput. Commun.*, vol. 101, pp. 69–81, 2017.

[37] S. Wang, W. Gao, and A. P. S. Meliopoulos, “An alternative method for power system dynamic state estimation based on unscented transform,” *IEEE Trans. Power Syst.*, vol. 27, no. 2, pp. 942–950, May 2012.
[38] J. Zhao, “Power system dynamic state estimation considering measurement correlations,” *IEEE Trans. Energy Convers.*, vol. 32, no. 4, pp. 1630–1632, Dec. 2017.
[39] A. K. Singh and B. C. Pal, “Decentralized dynamic state estimation in power systems using unscented transformation,” *IEEE Trans. Power Syst.*, vol. 29, no. 2, pp. 794–804, Mar. 2014.
[40] J. Hartikainen, A. Solin, and S. Särkkä, “Optimal filtering with Kalman filters and smoothers—A manual for matlab toolbox EKF/UKF,” *Biomed. Eng.*, pp. 1–57, 2008, [Online]. Available: https://www.cic.ipn.mx/~pescamilla/Sensor_Fusion/software/ManualKFToolBox.pdf.
[41] G. Valverde and V. Terzija, “Unscented Kalman Filter for power system dynamic state estimation,” *IET Gener., Transmiss. Distrib.*, vol. 5, no. 1, pp. 29–37, 2011.
[42] A. L. Da Silva, M. Do Coutto Filho, and J. D. Queiroz, “State forecasting in electric power systems,” *Proc. IEE Proc. C. (Gener., Transmiss. Distrib.)*, vol. 130, no. 5, pp 237–244, 1983.
[43] M. E. Baran and F. F. Wu, “Network reconfiguration in distribution systems for loss reduction and load balancing,” *IEEE Trans. Power Del.*, vol. 4, no. 2, pp. 1401–1407, Apr. 1989.
[44] Z. Dong, F. Zhengcai, and Z. Liuchun, “An improved TS algorithm for loss-minimum reconfiguration in large-scale distribution systems,” *Electric Power Syst. Res.*, vol. 77, no. 5, pp. 685–694, 2007.
[45] R. D. Zimmerman, C. E. Murillo-Sánchez, and R. J. Thomas, “MATPOWER: Steady-state operations, planning, and analysis tools for power systems research and education,” *IEEE Trans. Power Syst.*, vol. 26, no. 1, pp. 12–19, Feb. 2011.

Yubin Wang received the B.S. degree in electrical engineering and automation from Shandong Agricultural University, Taian, China, in 2016, and the M.S. degree in electrical engineering from Beijing Jiaotong University, Beijing, China, in 2019. He is currently working toward the Ph.D. degree with the College of Electrical Engineering, Zhejiang University, Hangzhou, China. His research interests include state and parameter estimation and power system control and optimization.

Mingchao Xia (Senior Member, IEEE) received the B.S. and Ph.D. degrees in electrical engineering from Tsinghua University, Beijing, China, in 1998 and 2003, respectively. He is currently a Professor with the School of Electrical Engineering, Beijing Jiaotong University, Beijing, China. His research interests include energy internet, smart power distribution system control and optimization, power electronics in power distribution, and flexible load control.

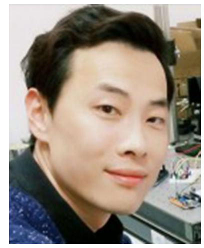

Qiang Yang (Senior Member, IEEE) received the Ph.D. degree in electronic engineering and computer science from the Queen Mary University of London, London, U.K., in 2007. From 2007 to 2010, he was with the Department of Electrical and Electronic Engineering, Imperial College London, London, U.K., and in 2015 and 2016, was a Visiting Scholar with the University of British Columbia, Vancouver, BC, Canada, and the University of Victoria, Victoria, BC, Canada. He is currently a Full Professor with the College of Electrical Engineering, Zhejiang University, Hangzhou, China. He has authored or cauthored more than 200 technical papers, applied 60 national patents, coauthored two books, and edited two books and several book chapters. His research interests include smart energy systems, large-scale complex network modeling, control and optimization, and learning-based optimization and control.

Prof. Yang is a Fellow of the British Computer Society and a Senior Member of China Computer Federation.

Yuguang Song (Graduate Student Member, IEEE) received the B.S. degree from Henan Polytechnic University, Henan, China, in 2016, and the M.S. degree from the School of Electrical Engineering, Beijing Jiaotong University, Beijing, China, in 2019. He is currently working toward the Ph.D. degree with the School of Electrical Engineering, Beijing Jiaotong University, Beijing, China. His research interests include demand response, smart grid, and load modeling.

Qifang Chen (Member, IEEE) received the B.S. degree in communication engineering and the M.S. degree in electric engineering from Xiangtan University, Xiangtan, China, in 2010 and 2013, respectively, and the Ph.D. degree in electrical engineering from North China Electric Power University, Beijing, China, in 2017. He is currently with the School of Electrical Engineering, Beijing Jiaotong University, Beijing, China. His research interests include integrated energy systems, demand response, and flexible load modeling and control.

Yuanyi Chen received the B.S. degree in electrical engineering from Beijing Jiaotong University, Beijing, China, in 2020. He is currently working toward the M.S. degree in electrical engineering with the Polytechnic Institute, Zhejiang University, Hangzhou, China. His research interests include feature aggregation and situation awareness of cyber-physical system with graph neural network.